Weak antilocalization of holes in HgTe quantum wells with a normal energy spectrum

G. M. Minkov,[1,2] A. V. Germanenko,[2] O. E. Rut,[2] A. A. Sherstobitov,[1,2] S. A. Dvoretski,[3] and N. N. Mikhailov[3]
[1]*M. N. Miheev Institute of Metal Physics of Ural Branch of Russian Academy of Sciences, 620137 Ekaterinburg, Russia*
[2]*Institute of Natural Sciences, Ural Federal University, 620002 Ekaterinburg, Russia*
[3]*Institute of Semiconductor Physics RAS, 630090 Novosibirsk, Russia*
(Received 9 December 2014; revised manuscript received 23 March 2015; published 6 May 2015)

The results of experimental study of quantum interference effects in small magnetic fields in narrow HgTe quantum wells of hole-type conductivity with a normal energy spectrum are presented. Interpretation of the data is performed with taking into account the strong spin-orbit splitting of the energy spectrum of the two-dimensional hole subband. It is shown that the phase relaxation time found from the analysis of the shape of magnetoconductivity curves in the case when the Fermi level lies in the monotonic part of the energy spectrum of the valence band behaves itself analogously to that observed in narrow HgTe quantum wells of electron-type conductivity. It increases in magnitude with the increasing conductivity and decreasing temperature following the $1/T$ law. Such a behavior corresponds to the inelasticity of electron-electron interaction as the main mechanism of the phase relaxation and agrees well with the theoretical predictions. For the higher conductivity, despite the fact that the dephasing time remains inversely proportional to the temperature, it strongly decreases with the increasing conductivity. It is presumed that the reason for such a peculiarity could be nonmonotonic character of the hole energy spectrum. An additional channel of inelastic interaction occurs when the Fermi level approaches the secondary maxima in the depth of the valence band.

DOI: 10.1103/PhysRevB.91.205302 PACS number(s): 73.20.Fz, 73.21.Fg, 73.63.Hs

I. INTRODUCTION

A new type of two-dimensional (2D) systems, in which energy spectrum is formed by the spin-orbit interaction, has attracted considerable interest during the last decade. The structures with a HgTe quantum well (QW) hold a special place among such structures. The strong intrinsic spin-orbit interaction leads to the energetic inversion of the Γ_8 and Γ_6 bands in bulk mercury telluride and to formation of a gapless band structure first proposed in Ref. [1] for gray tin. It results in nontrivial dependence of the energy gap on the width of the quantum well (d) and causes other important features of the energy spectrum of HgTe under spatial confinement. So the energy spectrum in the CdTe/HgTe/CdTe quantum well at $d = d_c \simeq 6.5$ nm is gapless [2] and is close to the linear Dirac-like spectrum at small quasimomentum (k) [3]. When the HgTe layer is thin, $d < d_c$, the ordering of energy subbands of spatial quantization is analogous to that in conventional semiconductors; the highest valence subband at $k = 0$ is formed from the heavy hole Γ_8 states, while the lowest electron subband is formed both from the Γ_6 states and light hole Γ_8 states. For a thick HgTe layer, $d > d_c$, the quantum well is in the inverted regime; the main electron subband is formed from the heavy hole Γ_8 states [4], whereas the subband formed from the Γ_6 states and light hole Γ_8 states sinks into the valence band. Besides, the energy spectrum of HgTe based heterostructures is very sensitive to a structure asymmetry due to strong Bychkov-Rasba effect [5].

The effects that depend not only on the energy spectrum, but on the wave functions also, have even more strong peculiarities. The interference contribution to the conductivity is just this effect. Suppression of interference by a magnetic field leads to arising of low-magnetic-field weak-localization (WL) or weak-antilocalization (WaL) magnetoconductivity (MC). Experimentally, the low field magnetoconductivity in 2D electron gas in HgTe QWs was observed in Refs. [6,7] and investigated in detail in Refs. [8,9]. There was shown [9] the phase relaxation time (τ_ϕ) increases with the temperature decrease as $1/T$, that corresponds to the case when inelasticity of electron-electron (e-e) interaction is the main dephasing mechanism [10]. It is important that the τ_ϕ value increases with increasing conductivity (σ) and this dependence is close to that predicted for this dephasing mechanism [11]: $\tau_\phi \propto \sigma/\ln(\sigma/G_0)$, where $\sigma \gg G_0 = e^2/(2\pi^2\hbar)$. Thus, the interference correction to the conductivity of 2D electron gas in HgTe QWs with $d < d_c$ behaves the same as that in conventional 2D systems with a simple energy spectrum [12].

Another behavior of τ_ϕ was observed for electrons in the structures with inverted spectrum, $d = (9$–$10)$ nm [8]. Whereas the temperature dependence of τ_ϕ remains conventional, $\tau_\phi \propto 1/T$, the σ dependence of τ_ϕ is strange: τ_ϕ is practically independent of conductivity. The reason for such a phenomenon is yet to be explained.

Concerning the weak localization in the hole 2D HgTe based systems, the theories [13–15] predict that the interference quantum correction for electrons and holes should be close to each other both for $d \lesssim d_c$ and $d \gtrsim d_c$. This is because the energy spectra of the valence bands near critical point d_c are very much like those of the conduction band for small quasimomentum values [3]. Despite the existence of a theoretical model and predictions, the weak localization in the hole HgTe QWs has not been experimentally studied to the best of our knowledge.

In this paper we present the results of an experimental investigation of the low-field magnetoconductivity in the gated HgTe quantum wells of hole-type conductivity with normal energy spectrum. Analyzing the shape of the MC curves we obtain the phase relaxation time within a wide conductivity range at different temperatures. We show that τ_ϕ increases in magnitude with the decreasing temperature following the $1/T$ law that is typical for the dephasing caused by inelastic e-e collisions. The conductivity dependence of

τ_ϕ at low conductivity, $\sigma \lesssim 100\,G_0$, is also usual for such a dephasing mechanism; the dephasing time increases with the increasing conductivity. For the higher conductivity, the behavior of τ_ϕ changes drastically. It strongly decreases with σ. The experimental results are discussed having regard to nonmonotonic character of the hole dispersion law.

II. EXPERIMENT

Our samples with HgTe quantum wells were realized on the basis of two HgTe/$Hg_{1-x}Cd_xTe$ ($x = 0.55$–0.65) heterostructures grown by molecular beam epitaxy on GaAs substrate with the (013) surface orientation [16]. The nominal width of the quantum well was 5.8 and 5.6 nm in the structures H724 and H1122, respectively. The quantum wells were of hole-type conductivity. The results for these structures are similar and we will mainly discuss the results which were obtained for the structure H724 with the higher Hall mobility. The samples were mesa etched into standard Hall bars of 0.5 mm width and the distance between the potential probes of 0.5 mm. To change and control the hole density (p) in the quantum well, the field-effect transistors were fabricated with parylene as an insulator and aluminum as a gate electrode. For each heterostructure, four samples were fabricated and studied. The hole density was about 1×10^{11} cm^{-2} for zeroth gate voltage in the heterostructure H724 and something less in H1122. The measurements were performed at temperatures of 1.3–4.2 K.

III. RESULTS AND DISCUSSION

The WL correction and MC curves depend not only on the momentum-, phase-, and spin-relaxation times but on the energy spectrum also. Therefore, before discussing the low-field magnetoconductivity let us look at the hole energy spectrum of the structures under study that was restored when analyzing the data of the transport measurements in Ref. [17].

The gate voltage dependence of the Hall density, $p_H = 1/[eR_H(0.1\ \mathrm{T})]$, where R_H is the Hall coefficient $R_H = \rho_{xy}/B$, and the hole densities that were found from analysis of Shubnikov–de Haas (SdH) oscillations are shown in Fig. 1(a). One can see that p_H linearly changes with V_g with a slope dp_H/dV_g of about -1.5×10^{10} cm^{-2} V^{-1} at $-2.5 < V_g <$

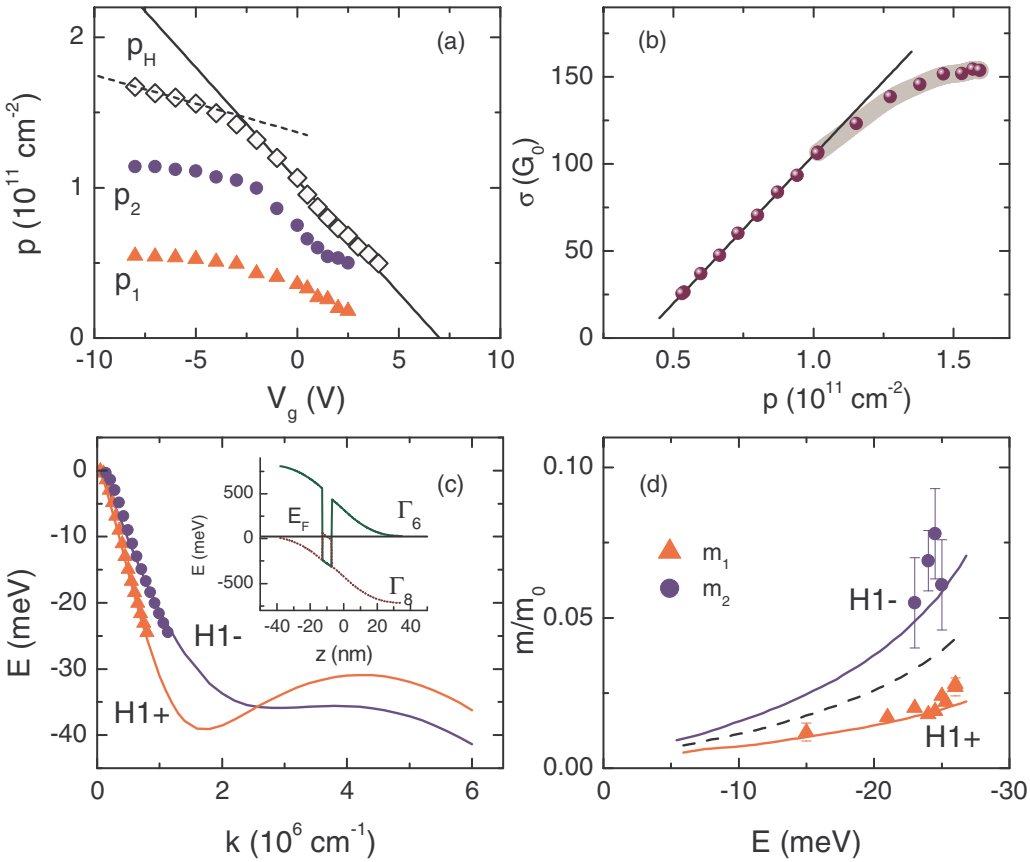

FIG. 1. (Color online) (a) The gate voltage dependence of the Hall density $p_H = 1/[eR_H(0.1\ \mathrm{T})]$ (diamonds) and densities p_1 and p_2 (triangles and circles, respectively) in the split subbands found from the SdH oscillations (for more details, see Ref. [17]). The solid line is drawn with the slope -1.5×10^{10} cm^{-2} V^{-1}, the dotted line is provided as a guide to the eye. (b) The conductivity plotted against the hole density. The data shadowed correspond to the regime where τ_ϕ drops with the increasing conductivity [see. Fig. 5(a)]. (c) The energy spectrum of the valence band. Symbols are restored from the experimental data [17]. The lines are the results of theoretical calculations with taking into account the electric field in the well. The inset shows the energy diagram of the structure calculated under the assumption that acceptor and donor densities in the lower and upper barriers are 3×10^{17} cm^{-3}. (d) The energy dependencies of the effective masses for the H1+ and H1− hole subbands. The symbols are the data [17] and the solid lines are the calculation results. The dashed curve is the average value of the effective mass $m_{av} = (m_1 + m_2)/2$.

4 V, where the hole density is less than $\simeq 1.5 \times 10^{11}$ cm^{-2}. At $V_g \lesssim -3.5$ V, the slope becomes much less. Note that capacitance between the gate electrode and the 2D channel measured on the same Hall bar is constant over the whole gate voltage range so that the value of $C/e = (1.4 \pm 0.15) \times 10^{10}$ cm^{-2} V^{-1} is very close to $|dp_H/dV_g| = 1.5 \times 10^{10}$ cm^{-2} V^{-1}. Analyzing these data together with the data obtained from the analysis of the temperature dependencies of the SdH oscillations amplitude, we have reconstructed the energy spectrum near the valence band top in Ref. [17]. These results are reproduced in Fig. 1(c). One can see first of all that the valence band is strongly split by spin-orbit interaction, so that the ratio of the hole densities in the split subbands is approximately equal to two. The energy spectrum is strongly nonparabolic, i.e., the hole effective masses significantly increases with the energy increase [Fig. 1(d)]. These results are well described within the framework of the kP model if one supposes that the lower barrier remains of p type, while the upper one is converted to n type after the growth stops, so that the quantum well is located in a strong electric field of p-n junction. The other key feature of the calculated spectrum is the secondary maxima located at $k \simeq 4 \times 10^6$ cm^{-1} at an energy distance of about 30 meV from the main maximum. As suggested in Ref. [17] these maxima can be responsible for flattening of the V_g dependence of the hole density at $V_g \lesssim -3.5$ V. Because of significantly larger density of states in the secondary maxima (as compared with that in central maximum) the sinking speed of the Fermi level decreases strongly when these states are being occupied at $V_g < -3.5$ V. In the presence of potential fluctuations, these states are localized due to large effective mass and, hence, do not contribute to the conductivity and the Hall effect. In this case, the Hall density will correspond to the hole density in the main maximum, while the total charge of carriers in the well will be determined by the density in all the maxima.

Now we are in position to analyze the low-field magnetoconductivity $\Delta\sigma(B) = 1/\rho_{xx}(B) - 1/\rho_{xx}(0)$. The experimental dependencies $\Delta\sigma(B)$ measured at different conductivity values are shown in Fig. 2(a). It is seen that the negative magnetoconductivity (antilocalization behavior) is observed at a low magnetic field. In the higher magnetic field, MC reverses the sign demonstrating the localization behavior.

It is well known that the characteristic field for the weak localization is a transport magnetic field $B_{tr} = \hbar/(2el^2) = \pi^3\hbar p/e \times (G_0/\sigma)^2$, with l as the transport mean free path, therefore in Fig. 2(b) we have plotted $\Delta\sigma$ against $b = B/B_{tr}$ (the use of one-type-carrier approximation in analyzing a weak antilocalization magnetoconductivity in the case of strong spin-orbit splitting is justified in Appendix A 2). As evident the crossover from the antilocalization to localization behavior of magnetoconductivity takes place at $b \gtrsim 1$ for all the conductivity values. In the following, we will analyze only the antilocalization magnetoconductivity, because the run of the MC curve beyond the diffusion regime, i.e., at $b > 1$, is not universal and strongly depends on scattering details, e.g., anisotropy of scattering probability and correlation in the scatterer distribution [18].

The quantitative analysis of the magnetic field dependence of the conductivity resulting from the suppression of the interference correction by the magnetic field is not a simple

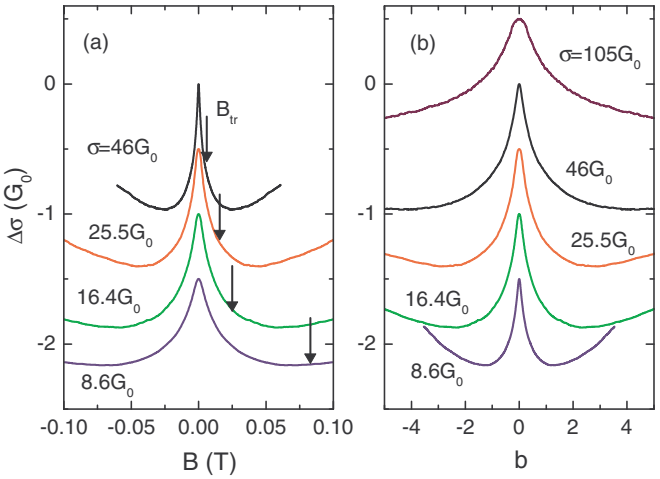

FIG. 2. (Color online) (a) The magnetic field dependencies of $\Delta\sigma$ for different conductivity values at $T = 1.35$ K. The arrows show the values of B_{tr}. (b) The same data plotted against the relative magnetic field $b = B/B_{tr}$. For clarity, the curves are shifted in the vertical direction.

problem for our case because the valence band is strongly split by spin-orbit interaction. Since the hole effective masses in split subbands are different, the mobilities can be different and, hence, the transport magnetic fields as well as the τ to τ_ϕ ratio can be different also. To the best of our knowledge, the WL magnetoconductivity for such a specific situation is as yet not calculated. However, there are two limiting cases when the expression for the magnetoconductivity can be obtained from qualitative considerations: (i) the transitions between subbands are slow in the sense that $\tau_{12} \gg \tau_\phi$, where τ_{12} is the transition time, and (ii) they are fast, $\tau_{12} \ll \tau_\phi$.

In the first case, $\tau_{12} \gg \tau_\phi$, the total WL magnetoconductivity is simply the sum of independent contributions from each split subbands:

$$\Delta\sigma = \Delta\sigma_1 + \Delta\sigma_2. \quad (1)$$

Here $\Delta\sigma_1$ and $\Delta\sigma_2$ are antilocalizing [19] because the carrier spin is rigidly coupled with the momentum in the systems under study. Then, Eq. (1) in the diffusion regime ($b \ll 1$, $\tau \ll \tau_\phi$) may be written as follows:

$$\Delta\sigma = -\frac{G_0}{2}\left[\mathcal{H}\left(\frac{B}{B_{tr}^{(1)}}, \frac{\tau_1}{\tau_\phi^{(1)}}\right) + \mathcal{H}\left(\frac{B}{B_{tr}^{(2)}}, \frac{\tau_2}{\tau_\phi^{(2)}}\right)\right], \quad (2)$$

where

$$\mathcal{H}(b,x) = \psi\left(\frac{1}{2} + \frac{x}{b}\right) - \psi\left(\frac{1}{2} + \frac{1}{b}\right) - \ln x$$
$$\simeq \psi\left(\frac{1}{2} + \frac{x}{b}\right) - \ln\left(\frac{x}{b}\right), \quad b \lesssim 1,$$

$\psi(x)$ is a digamma function, and $i = 1,2$ numbers the split subbands. Obviously it is impossible to reliably find the dephasing times while fitting the smooth curve, if the subband parameters entering Eq. (2) are strongly different and unknown independently with high enough accuracy. It becomes possible only when the corresponding parameters of subbands are close to each other. Then, in the first approximation, Eq. (2) is

reduced to

$$\Delta\sigma = \alpha G_0 \mathcal{H}\left(\frac{B}{B_{\rm tr}}, \frac{\tau}{\tau_\phi}\right), \quad (3)$$

with $\alpha \simeq -1$, which can be already used to find τ_ϕ.

If a carrier executes many transitions between subbands within the phase breaking time, i.e., $\tau_{12} \ll \tau_\phi$, the magnetoconductivity has the same form [Eq. (3)] in which, however, the prefactor α is equal to $-1/2$ instead of -1, and the parameters $B_{\rm tr}$, τ, and τ_ϕ are averages over two subbands [20–22]. Qualitatively, this can be explained by the fact that the probability of return to the starting point after traveling over closed path, while remaining in the same subband, is reduced by half.

Our analysis of the magnetic field dependencies of the Hall coefficient performed within classical magnetic field range in Appendix A 1 allows us to estimate the hole densities and mobilities in the different split subbands and, thus, estimate the τ_i and $B_{\rm tr}^{(i)}$ values. It turns out that the values of $\tau_1 B_{\rm tr}^{(1)}$ and $\tau_2 B_{\rm tr}^{(2)}$, which determined the run of the MC curve at $b < 1$ [see Eq. (2)], are close to each other within accuracy better than 30% over the whole conductivity range. Besides, simulating the WaL MC curves we show in Appendix A 2 that the use of a one-band formula [Eq. (3)] allows us to obtain the dephasing rate with accuracy better than 10% both for $\tau_{12} \ll \tau_\phi$ and $\tau_{12} \gg \tau_\phi$. Thus, the use of Eq. (3) for the data analysis seems warranted in our case.

Let us now consider the fitting results. In Fig. 3(a) we present as an example the data measured for $\sigma = 46.0\,G_0$ together with the fitting curve. The fit has been made within the magnetic field range $b = 0$–0.3. The parameters α and $\tau/\tau_\phi = x$ in Eq. (3) have been used as the fitting ones. The dephasing time has been estimated with the use of the total conductivity and hole density σ and p, respectively, and average effective mass $m_{\rm av}$ as follows: $\tau_\phi = \tau/x$, where $\tau = \sigma m_{\rm av}/(e^2 p)$, $m_{\rm av} = (m_1 + m_2)/2$ [see Fig. 1(d)]. It is evident that Eq. (3) describes the MC curve rather well.

It should be mentioned that the values of the fitting parameters are somewhat sensitive to the width of the fitting b interval as Figs. 3(b) and 3(c) illustrate. The dephasing time τ_ϕ increases while the prefactor α slightly decreases in magnitude with the expanding interval. This can be partially attributed to the fact that the diffusion regime $\tau \ll \tau_\phi$ is not strictly satisfied under our experimental conditions: τ_ϕ is only 10–30 times larger than τ depending upon the conductivity and temperature. As shown in Appendix B the values of the fitting parameters are really dependent on the fitting interval if the diffusion formula, Eq. (3), is used for description of the MC curve beyond the diffusion regime. From the dashed curves in Figs. 3(b) and 3(c) it is evident that the experimental and theoretical dependencies are qualitatively similar. The fact that the fitting value of α is close to -0.5 indicates that the transition time between the split subbands is less than the dephasing time, $\tau_{12} < \tau_\phi$.

Now, let us inspect Fig. 4, in which the temperature dependencies of τ_ϕ and α are presented. It is seen that τ_ϕ varies as $1/T$, as it should be when the inelasticity of e-e interaction is responsible for dephasing. But the prefactor α changes with the temperature also. Such temperature dependence of α is described quite well when one takes into account the decrease of τ_ϕ/τ with the temperature increase [see dashed curve in Fig. 4(b)], which worsens applicability of the diffusion approximation (see Appendix B).

Thus, a sufficiently good agreement of the theoretical MC curve with the experimental one, the conventional behavior of the fitting parameter τ_ϕ with the temperature, and understandable behavior of α, all this together testifies the adequacy of the used model to find the value of τ_ϕ.

The same treatment has been applied to data analysis at different gate voltages, that allows us to obtain experimentally

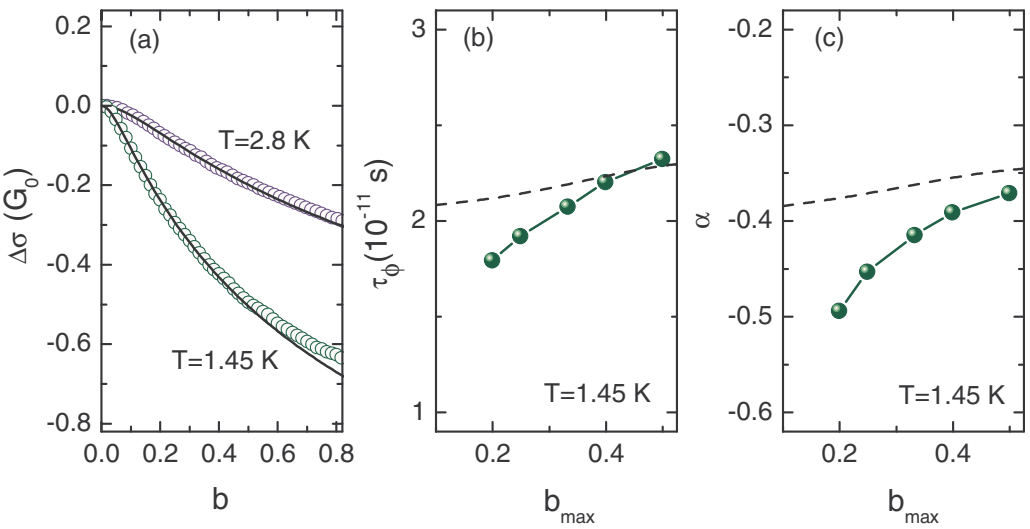

FIG. 3. (Color online) (a) The magnetic field dependence of $\Delta\sigma$ for $\sigma = 46.0\,G_0$ at $T = 1.45$ and 2.8 K. Symbols are the experimental data and the curves are the best fit to Eq. (3) made within the magnetic field range $b = (0 - b_{\rm max})$, $b_{\rm max} = 0.3$. (b) and (c) The dependence of the fitting parameters τ_ϕ and α, respectively, on the upper limit of the fitting magnetic field range $b_{\rm max}$. The dashed curves in (b) and (c) are the fitting parameters plotted against $b_{\rm max}$ as they are obtained when Eq. (3) is used to fit the MC curve calculated for $\tau_\phi = 2 \times 10^{-11}$ s and $\tau_\phi/\tau = 30$ in the framework of the model valid beyond the diffusion regime (for more details, see Appendix B).

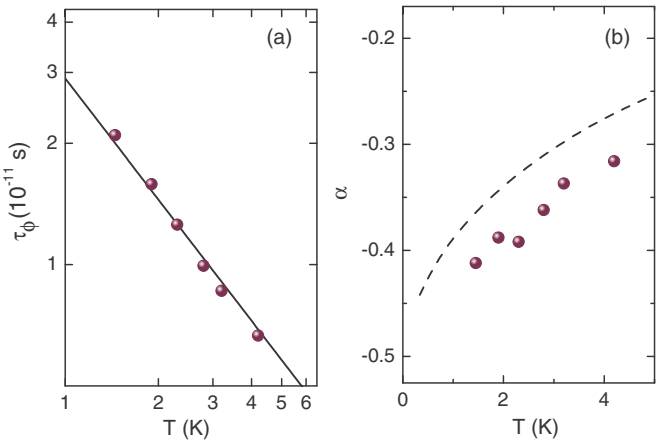

FIG. 4. (Color online) The temperature dependencies of the fitting parameters τ_ϕ (a) and α (b) found in the fitting interval $b = 0$–0.3 for $p = 7.9 \times 10^{10}$ cm^{-2}, $\sigma = 63\,G_0$. Straight line in (a) is the dependence $\tau_\phi = 2.9 \times 10^{-11}/T$ s. The dashed curve in (b) is α plotted against T as it is obtained when the diffusion expression Eq. (3) is used within the range $b = (0$–$0.3)$ for the fit of the MC curve calculated beyond the diffusion approximation (see Appendix B).

the conductivity dependence of τ_ϕ and α over the whole conductivity range $\sigma = (5$–$150)\,G_0$.

Let us discuss the conductivity dependence of the phase relaxation time. The theory [11] predicts that τ_ϕ should increase with the conductivity when the inelasticity of *e-e* interaction is the main mechanism of the dephasing. Such a prediction is justified in experiments on the quantum wells with ordinary spectrum (see, e.g., Ref. [12], where the data for GaAs/In$_{0.2}$Ga$_{0.8}$As/GaAs quantum well are presented).

The experimental dependence $\tau_\phi(\sigma)$ measured at $T = 1.35$ K is shown in Fig. 5(a). First, we consider the region where the conductivity is less than $\simeq 100\,G_0$ (this corresponds

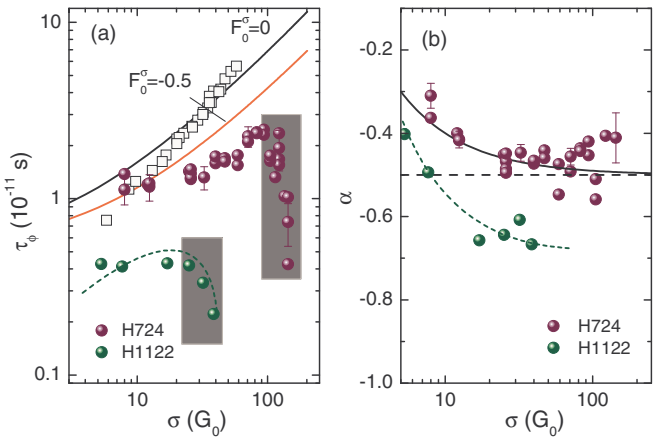

FIG. 5. (Color online) The conductivity dependence of τ_ϕ (a) and α (b) for two heterostructures under study (spheres), $T = 1.35$ K. The squares are the data from Ref. [9] relating to the electron gas in the HgTe QW with $d = 5$ nm. The solid curves in (a) are calculated according to Ref. [11]. The shadow areas indicate the drops in the τ_ϕ vs σ dependencies. The solid curve in (b) is the dependence $-0.5 \times (1 - 2\,G_0/\sigma)$ [12]. The dotted lines are provided as a guide to the eye.

to the case when the distance between the valence band top and Fermi level is less than 20–25 meV). It is evident that τ_ϕ increases with the conductivity within this conductivity range. Such a behavior agrees rather well with the theoretical prediction [11]. The absolute values of τ_ϕ are also in satisfactory agreement with the theoretical results obtained in Ref. [11] that is clearly seen from Fig. 5, where the solid curves represents the calculation results for two values of the parameter of *e-e* interaction F_0^σ: $F_0^\sigma = 0$ and $F_0^\sigma = -0.5$.

Note that the second fitting parameter α somewhat decreases in absolute value with the decreasing conductivity [Fig. 5(b)]. Such a behavior is also natural and is in reasonable agreement with the behavior of α in conventional two-dimensional systems and with the theoretical dependence obtained with taking into account second loop corrections: $\alpha(\sigma) = \alpha(\sigma \to \infty)(1 - 2\,G_0/\sigma)$ [12], where $\alpha(\sigma \to \infty) = -1/2$ for our case.

It is appropriate to recall that the conductivity dependencies of τ_ϕ for electrons in HgTe QWs were investigated in Refs. [8,9]. It was found that they were different in the quantum wells with inverted ($d > d_c$) and normal ($d < d_c$) spectra. So the dephasing time of electrons increased with growing σ at $d < d_c$ [9]. Figure 5(a) shows that the dephasing time of the holes in the structures investigated in the present paper [with $d = (5.6$–$5.8)$ nm $< d_c$] behaves the same. This is different from that observed for electrons in the structures with the inverted spectrum, where τ_ϕ was practically independent of σ [8]. The interference correction for holes with the inverted spectrum still remains to be studied.

Thus, the interference quantum correction to the conductivity in the HgTe quantum well with normal spectrum, $d < d_c$, both for electrons and for holes, is analogous to that in ordinary 2D systems. Namely, the magnetoconductivity curves are well described by the conventional expression Eq. (3). The temperature and conductivity dependencies of τ_ϕ found from the fit to Eq. (3) are more or less close to the theoretical ones derived for the case when inelasticity of *e-e* interaction is the main dephasing mechanism.

Let us now consider the dephasing time at higher conductivity ($\sigma > 100\,G_0$) that corresponds to the hole density larger than 1×10^{11} cm^{-2} for the structure H724. It is seen from Fig. 5(a) that the value of τ_ϕ decreases abruptly with the conductivity increase. As Fig. 1(a) shows the hole density 1×10^{11} cm^{-2} is close to though somewhat less than the value at which the increase of the hole density begins to slow down with the increasing negative gate voltage. This suggests that both these facts are of common origin. The analogous behavior of the conductivity dependence of τ_ϕ is observed in the structure H1122 (see Fig. 5), in which the change of slope in the p_H vs V_g dependence occurs at the lower hole density $p \simeq 1.1 \times 10^{11}$ cm^{-2}. Since the change in dp_H/dV_g at low V_g values is possibly caused by the population of the secondary maxima in the valence band spectrum [see Fig. 1(c)], it is reasonable to assume that the appearance of the carriers in the secondary maxima leads to occurrence of an additional mechanism of the phase relaxation.

Another possibility to explain the feature under discussion is the existence of localized states in the lower barrier which start to be occupied with the decreasing gate voltage leading to the same effect in the dependence $p(V_g)$ at $p \simeq 1 \times 10^{11}$ cm^{-2}.

Inelasticity of the interaction with carriers in these states may also result in the sharp decrease of τ_ϕ. We cannot exclude this mechanism at the moment.

IV. CONCLUSION

The results of experimental study of the interference quantum correction to the conductivity in the narrow quantum well HgTe of the hole type with the normal energy spectrum are presented. Analysis of the interference-induced low-field magnetoconductivity has been performed with taking into account the strong spin-orbit splitting of the hole subband. We have shown that the temperature dependence of the phase relaxation time found from the fit of the magnetoconductivity curves is close to $1/T$ over the whole conductivity range $\sigma = (5\text{–}150)\,G_0$. Such a behavior is typical for the dirty two-dimensional systems at low temperature when the inelasticity of electron-electron interaction is the main dephasing mechanism.

The conductivity dependence of the phase relaxation times is nonmonotonic, which may be a consequence of nonmonotonic dispersion $E(k)$ of the main hole subband of spatial quantization. At relatively low conductivity ($\sigma < 100\,G_0$ for the quantum well of 5.8 nm width), when the Fermi level lies above the secondary maxima of the dispersion, the dephasing time increases with the conductivity increase analogously to that observed for electrons in narrow HgTe quantum wells with the normal energy spectrum [9] and in ordinary single quantum wells. Such a behavior is in agreement with that predicted theoretically [11] for the case when inelasticity of *e-e* interaction is responsible for the phase relaxation. The τ_ϕ decrease evident at higher conductivity $\sigma > 100\,G_0$, when the Fermi level is close or even arrives the secondary maxima, may result from the additional channel of the inelastic interaction.

ACKNOWLEDGMENTS

We are grateful to I. V. Gornyi, V. Yu. Kachorovskii, and P. M. Ostrovsky for useful discussions. The work has been supported in part by the Russian Foundation for Basic Research (Grants No. 13-02-00322 and No. 15-02-02072) and the Russian Academy of Sciences (Project No. 12-P-2-1051). A.V.G. and O.E.R. gratefully acknowledge financial support from the Ministry of Education and Science of the Russian Federation under Projects No. 3.571.2014/K and No. 2457.

APPENDIX A: APPLICABILITY OF THE ONE-TYPE-CARRIER APPROXIMATION TO ANALYSIS OF WEAK ANTILOCALIZATION MAGNETOCONDUCTIVITY

1. Estimations of τ and B_{tr} in subbands

The valence band in the systems under study is strongly split by spin-orbit interaction due to asymmetry of the quantum well. In order to obtain the phase relaxation time in such a situation we need to know the transport relaxation times τ_i and transport magnetic fields $B_{\rm tr}^{(i)}$, where $i = 1,2$ numbers the split subband.

The τ_i and $B_{\rm tr}^{(i)}$ values can be estimated from analysis of the experimental magnetic field dependencies of ρ_{xx} and

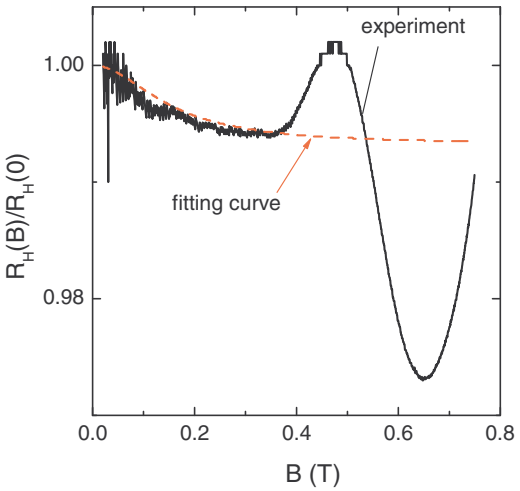

FIG. 6. (Color online) The magnetic field dependence of $R_{\rm H}(B)/R_{\rm H}(0)$ for $\sigma = 58.7\,G_0$ (structure H724). The solid curve is experimental and the dashed one is the result of the best fit with the parameters given in Table I.

$R_{\rm H}$ at classical magnetic field $\mu_i B < 1$, within framework of the standard model of conductivity by two types of carriers. Because there are additional mechanisms of the magnetic field dependence of ρ_{xx} (e.g., the quantum correction due to *e-e* interaction), we have analyzed only the dependence $R_{\rm H}(B)$. It has been fitted to the classical textbook expression for the Hall coefficient [23] with the use of mobilities μ_1 and μ_2 as the fitting parameters, and p_1 and p_2 which were found from the SdH oscillations [see Fig. 1(a)]. As an example we present the results of such a fit for $\sigma = 58.7\,G_0$ in Fig. 6. All the parameters used in and found from the fit are listed in Table I. The transport relaxation times τ_i were found as $\tau_i = \mu_i m_i/e$, with m_1 and m_2 from Fig. 1(d). The transport magnetic fields have been calculated as $B_{\rm tr}^{(i)} = \hbar/(2el_i^2) = \pi^3\hbar p_i/(2e) \times (G_0/\sigma_i)^2$.

Although as seen from Fig. 6 the fit quality is quite good, the accuracy in determination of the fitting parameters is not very high. This is because the variation of the Hall coefficient in the magnetic field is less than 1% and the experimental $R_{\rm H}$

TABLE I. The parameters of the different split subbands for $\sigma = 58.7\,G_0$.

	$i = 1$		$i = 2$
p_i (10^{10} cm^{-2})[a]	2.4		4.8
μ_i (10^4 cm^2/V s)[b]	7.0		5.9
m_i/m_0	0.012		0.028
τ_i (10^{-13} s)	4.8		9.4
$B_{\rm tr}^{(i)}$ (mT)	5.1		3.6
B_{tr} (mT)		4.3	
τ_ϕ (10^{-11} s)		2.0	
$\tau_\phi^{\rm fit}$ (10^{-11} s)		2.17	
$\alpha^{\rm fit}$		−0.98	

[a]Found from the SdH oscillations.
[b]Obtained from the fit of $R_{\rm H}$ vs B data.

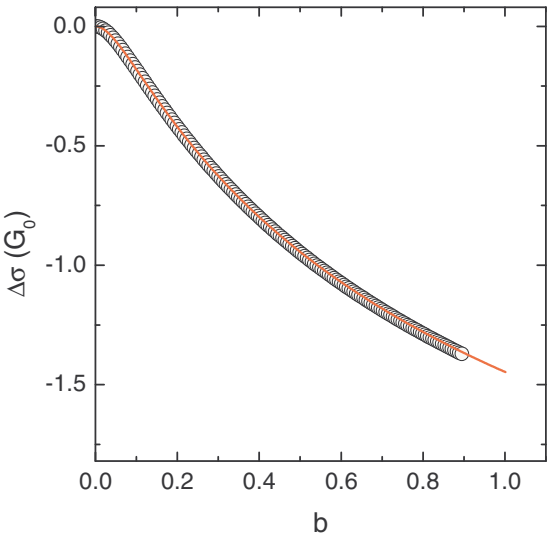

FIG. 7. (Color online) The magnetoconductivity plotted as a function of $b = B/B_{tr}$. The symbols are calculated from Eq. (2), the curves are results of the best fit by Eq. (3) within the b range from 0 to 0.3. The parameters are given in Table I.

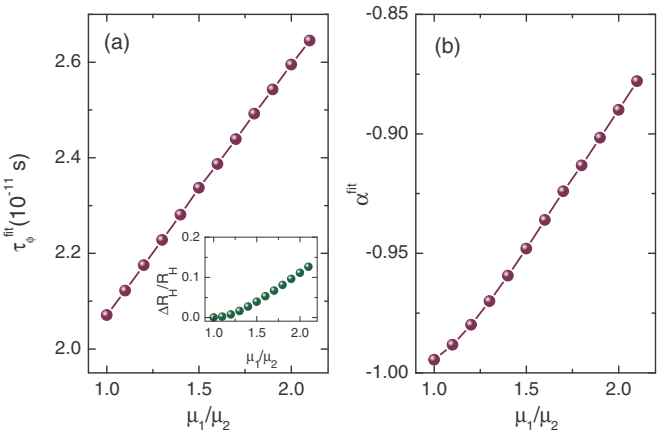

FIG. 8. (Color online) The fitting parameters τ_ϕ^{fit} (a) and α^{fit} (b) plotted against the μ_1 to μ_2 ratio.

vs B traces are noisy on this scale. For this concrete case, we estimate the error by the value $\pm 20\%$.

2. Estimation of errors at using one-band approximation for analysis of WL MC

Let us estimate an error in determination of the τ_ϕ and α values, which arises if one uses "one-band" expression Eq. (3) to fit the data for the case of two strongly split subbands.

We start with the case of slow transitions between the subbands ($\tau_{12} \gg \tau_1, \tau_2$). We have calculated the interference correction to the conductivity using Eq. (2) with the parameters from Table I. Therewith, we have supposed $\tau_\phi^{(1)} = \tau_\phi^{(2)} = \tau_\phi$ because the dephasing time is determined by conductivity under conditions that inelasticity of e-e collisions is responsible for dephasing. Then the calculated $\Delta\sigma$ vs B curve has been processed the same way as experimental data, i.e., fitted to Eq. (3), in which $B_{tr} = \pi^3 \hbar p/e \times (G_0/\sigma)^2$, $\tau = \sigma m/(e^2 p)$, where p stands for the total hole density $p_1 + p_2$, σ is the total conductivity, and $m = (m_1 + m_2)/2$. The parameters α and τ_ϕ have been used as the fitting ones. It is evident from Fig. 7 that Eq. (3) describes the simulated dependence $\Delta\sigma(B)$ very well. As seen from Table I the τ_ϕ^{fit} value is close to τ_ϕ used in calculation: $\tau_\phi^{fit} \simeq 2.2 \times 10^{-11}$ s against $\tau_\phi = 2.0 \times 10^{-11}$ s. The fitting value of the prefactor is equal to -0.98 that practically coincides with -1.

Since the accuracy in obtaining mobilities is not high under our experimental conditions, it is useful to estimate how strongly the fitting parameters τ_ϕ^{fit} and α^{fit} depend on the μ_1 to μ_2 ratio. For this purpose we have calculated the set of the magnetoconductivity curves $\Delta\sigma(B)$ with $\tau_\phi = 2 \times 10^{-10}$ s for the different μ_1 to μ_2 ratio values while keeping $n_1 = 2.4 \times 10^{10}$ cm^{-2}, $n_2 = 4.8 \times 10^{10}$ cm^{-2}, and $\sigma = 58.7\, G_0$. Note the change of the Hall coefficient in the magnetic field $\Delta R_H/R_H = [R_H(0) - R_H(\infty)]/R_H(0)$ does not exceed 15% therewith [see the inset in Fig. 8(a)]. Then, we have performed the fitting procedure within the b range from 0 to 0.3. The parameters τ_ϕ^{fit} and α^{fit} corresponding to the best fit are presented in Figs. 8(a) and 8(b), respectively. It is seen that the error in determination of τ_ϕ does not exceed 30%, while the μ_1 to μ_2 ratio varies within the relatively wide interval: $\mu_1/\mu_2 \simeq 1$–2. The value of α^{fit} remains always close to -1.

As for the case of fast transitions between subbands ($\tau_{12} \ll \tau_1, \tau_2$), $\Delta\sigma(B)$ in the diffusion regime is given by Eq. (3) with $\alpha = -1/2$, which in slightly different form can be written as follows [20–22]:

$$\Delta\sigma = -\frac{G_0}{2}\left[\psi\left(\frac{1}{2} + \frac{4eD_0\tau_\phi'}{\hbar B}\right) - \ln\left(\frac{4eD_0\tau_\phi'}{\hbar B}\right)\right], \quad \text{(A1)}$$

where

$$\frac{1}{\tau_\phi'} = \frac{\nu_1/\tau_\phi^{(1)} + \nu_2/\tau_\phi^{(2)}}{\nu_2 + \nu_2},$$

$$D_0 = \frac{\nu_1 D_1 + \nu_2 D_2}{\nu_2 + \nu_2} = \frac{\pi\hbar^2\sigma}{e^2}\frac{2}{m_1 + m_2}.$$

Here $\nu_i = m_i/2\pi\hbar^2$ are the densities of states and $D_i = \sigma_i/e^2\nu_i$ are the diffusion constants for ith subband ($i = 1,2$). As seen the fitting procedure has to give the value of τ_ϕ' (or τ_ϕ when $\tau_\phi^{(1)} = \tau_\phi^{(2)} = \tau_\phi$) exactly if one uses the average effective mass $m = (m_1 + m_2)/2$ in the standard expression for the diffusion constant $D = \pi\hbar^2\sigma/(e^2 m)$.

Thus, we conclude that the use of Eq. (3) for description of the interference induced magnetoconductivity is justified under our experimental conditions. Therefore, the fitting procedure allows us to obtain not only the value of the phase relaxation time but to estimate the rate of intersubband transitions. If the value of α^{fit} is close to $-1/2$, $\tau_{12} \ll \tau_\phi$. When $\alpha^{fit} \simeq -1$, $\tau_{12} \gg \tau_\phi$.

APPENDIX B: WORKABILITY OF THE DIFFUSION FORMULA BEYOND DIFFUSION REGIME

Equations (2) and (3) are valid in the diffusion regime, i.e., when both of the two conditions $B \ll B_{tr}$ and $\tau_\phi \gg \tau$ are satisfied. The calculation of WL MC beyond the diffusion regime

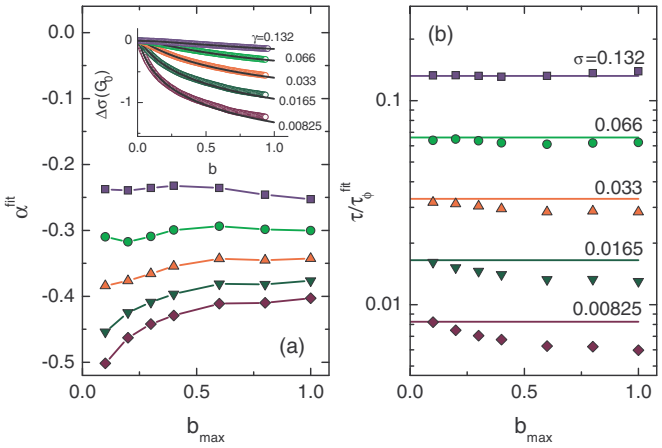

FIG. 9. (Color online) The fitting parameters α^{fit} (a) and $\tau/\tau_\phi^{\text{fit}}$ (b) plotted against the width of the magnetic field range, in which the fit of the data presented in the inset in (a) has been done. In the inset: Symbols are obtained from the numerical simulation with different values of $\gamma = \tau/\tau_\phi$; the curves are the results of the best fit by Eq. (3) within the range $b = (0 - b_{\max})$, $b_{\max} = 0.3$.

was carried out in a number of papers (e.g., in Refs. [24–28]). However, the expressions obtained are so cumbersome that it is difficult to use them for the fit of experimental curves. In order to estimate how well the fitting parameters are obtained when Eq. (3) is used for the description of the MC curve if the conditions of the diffusion regime are not strictly satisfied, we have used the numerical simulation approach developed in Ref. [29]. The "experimental" curves have been calculated with the use of Eq. (21) from that paper. In order to take into account the fast transitions between subbands $\tau_{12} \ll \tau_\phi$, the right-hand side of this equation has been multiplied by the factor $-1/2$ (for more details, see Ref. [30]). The simulated data for different values of $\gamma = \tau/\tau_\phi$ and fitting curves are presented in the inset in Fig. 9(a). It is evident that the data are fitted by Eq. (3) perfectly. As Figs. 9(a) and 9(b) illustrate the values of the fitting parameters α and τ/τ_ϕ are sensitive to the width of the magnetic field range $(0 - b_{\max})$, in which the fit is performed. However, inspection of Fig. 9(b) shows that the relative difference between the $\tau/\tau_\phi^{\text{fit}}$ values and the values τ/τ_ϕ used in the simulation procedure does not exceed 10%, if one restricts the fitting interval by the value $b_{\max} = 0.3$.

[1] S. Groves and W. Paul, Phys. Rev. Lett. **11**, 194 (1963).

[2] L. G. Gerchikov and A. Subashiev, Phys. Status Solidi (b) **160**, 443 (1990).

[3] B. A. Bernevig, T. L. Hughes, and S.-C. Zhang, Science **314**, 1757 (2006).

[4] M. I. D'yakonov and A. Khaetskii, Zh. Eksp. Teor. Fiz. **82**, 1584 (1982) [Sov. Phys. JETP **55**, 917 (1982)].

[5] Y. A. Bychkov and E. I. Rashba, J. Phys. C: Solid State Phys **17**, 6039 (1984).

[6] E. B. Olshanetsky, Z. D. Kvon, G. M. Gusev, N. N. Mikhailov, S. A. Dvoretsky, and J. C. Portal, Pis'ma Zh. Eksp. Teor. Fiz. **91**, 375 (2010) [JETP Lett. **91**, 347 (2010)].

[7] M. Mühlbauer, A. Budewitz, B. Büttner, G. Tkachov, E. M. Hankiewicz, C. Brüne, H. Buhmann, and L. W. Molenkamp, Phys. Rev. Lett. **112**, 146803 (2014).

[8] G. M. Minkov, A. V. Germanenko, O. E. Rut, A. A. Sherstobitov, S. A. Dvoretski, and N. N. Mikhailov, Phys. Rev. B **85**, 235312 (2012).

[9] G. M. Minkov, A. V. Germanenko, O. E. Rut, A. A. Sherstobitov, S. A. Dvoretski, and N. N. Mikhailov, Phys. Rev. B **88**, 045323 (2013).

[10] B. L. Altshuler and A. G. Aronov, in *Electron-Electron Interaction in Disordered Systems*, edited by A. L. Efros and M. Pollak (North Holland, Amsterdam, 1985), p. 1.

[11] B. N. Narozhny, G. Zala, and I. L. Aleiner, Phys. Rev. B **65**, 180202 (2002).

[12] G. M. Minkov, A. V. Germanenko, and I. V. Gornyi, Phys. Rev. B **70**, 245423 (2004).

[13] G. Tkachov and E. M. Hankiewicz, Phys. Rev. B **84**, 035444 (2011).

[14] P. M. Ostrovsky, I. V. Gornyi, and A. D. Mirlin, Phys. Rev. B **86**, 125323 (2012).

[15] I. V. Gornyi, V. Y. Kachorovskii, and P. M. Ostrovsky, Phys. Rev. B **90**, 085401 (2014).

[16] N. N. Mikhailov, R. N. Smirnov, S. A. Dvoretsky, Y. G. Sidorov, V. A. Shvets, E. V. Spesivtsev, and S. V. Rykhlitski, Int. J. Nanotechnol. **3**, 120 (2006).

[17] G. M. Minkov, A. V. Germanenko, O. E. Rut, A. A. Sherstobitov, S. A. Dvoretski, and N. N. Mikhailov, Phys. Rev. B **89**, 165311 (2014).

[18] A. V. Germanenko, G. M. Minkov, A. A. Sherstobitov, and O. E. Rut, Phys. Rev. B **73**, 233301 (2006).

[19] I. V. Gornyi, A. P. Dmitriev, and V. Y. Kachorovski, Pis'ma Zh. Eksp. Teor. Fiz. **68**, 314 (1998) [JETP Lett. **68**, 338 (1998)].

[20] N. S. Averkiev, L. E. Golub, and G. E. Pikus, Fiz. Tekh. Poluprovodn. **32**, 1219 (1998) [Semiconductors **32**, 1087 (1998)].

[21] O. E. Raichev and P. Vasilopoulos, J. Phys.: Condens. Matter **12**, 589 (2000).

[22] N. S. Averkiev, L. E. Golub, S. A. Tarasenko, and M. Willander, Phys. Rev. B **64**, 045405 (2001).

[23] F. J. Blatt, *Physics of Electronic Conduction in Solids* (McGraw-Hill, New York, 1968), p. 446.

[24] H.-P. Wittmann and A. Schmid, J. Low Temp. Phys. **69**, 131 (1987).

[25] A. P. Dmitriev, V. Y. Kachorovskii, and I. V. Gornyi, Phys. Rev. B **56**, 9910 (1997).

[26] A. Cassam-Chenai and B. Shapiro, J. Phys. I (France) **4**, 1527 (1994).

[27] L. E. Golub, Phys. Rev. B **71**, 235310 (2005).

[28] F. V. Porubaev and L. E. Golub, Phys. Rev. B **87**, 045306 (2013).

[29] G. M. Minkov, A. V. Germanenko, V. A. Larionova, S. A. Negashev, and I. V. Gornyi, Phys. Rev. B **61**, 13164 (2000).

[30] A. V. Germanenko, G. M. Minkov, O. Rut, and A. Sherstobitov, Int. J. Mod. Phys. **21**, 1669 (2007).